

Supplementary data for

How to design more efficient hole-transporting materials for perovskite solar cells? Rational tailoring of the triphenylamine-based electron donor

Yu-Lin Xu,[†] Wei-Lu Ding,[‡] and Zhu-Zhu Sun^{*,†}

[†]Energy-Saving Building Materials Innovative Collaboration Center of Henan Province, Xinyang Normal University, Xinyang, 464000, China

[‡]Beijing Key Laboratory of Photoelectronic/Electrophotonic Conversion Materials, Key Laboratory of Cluster Science of Ministry of Education, School of Chemistry, Beijing Institute of Technology, Beijing 100081, China

E-mail: Z.Z.Sun: zhuzhusun@xynu.edu.cn

Computational details

The geometry optimizations of the HTM/MAPbI₃ complexes were performed by the CP2K/QUICKSTEP program¹⁻³ combined with a hybrid Gaussian and plane wave basis set. The generalized-gradient approximation(GGA)⁴ of Perdew-Burke-Ernzerhof (PBE)⁵ exchange correlation functional was employed together with norm-conserving Goedecker-Teter-Hutter (GTH)⁶ pseudopotentials, and when forces were less than 45 meV Å⁻¹ (default value), the structures were considered as relaxed. Based on the optimized HTM/MAPbI₃ geometries, single-point DFT calculations were carried out with Gaussian 09 package to gain the electronic and energetic properties of HTM adsorbed systems at the theoretical level of B3LYP/6-31G*, coupled with the LANL2DZ potentials.⁷ Herein, the (MAPbI₃)₆₄ cluster was obtained by appropriately cutting a tetragonal phase slab with the (001) surface exposed,⁸ which was believed to favor the hole injection from MAPbI₃ to HTMs. Meanwhile, the parallel adsorption configuration⁹ was reported to be energetic favorable for HTMs with big π -conjugated cores, and thus this adsorption model was employed for the new designed NTT-4TPA.

References

1. J. Hutter, M. Iannuzzi, F. Schiffmann and J. VandeVondele, *WIRES Comput. Mol. Sci.*, 2014, **4**, 15-25.
2. J. VandeVondele, M. Krack, F. Mohamed, M. Parrinello, T. Chassaing and J. Hutter, *Comput. Phys. Commun.*, 2005, **167**, 103-128.
3. W. L. Ding, X. L. Peng, Z. Z. Sun and Z. S. Li, *Nanoscale*, 2017, **9**, 16806-16816.
4. J. P. Perdew, K. Burke and M. Ernzerhof, *Phys. Rev. Lett.*, 1996, **77**, 3865-3868.
5. K. Burke, J. P. Perdew and M. Ernzerhof, *Phys. Rev. Lett.*, 1997, **80**, 891.
6. C. Hartwigsen, S. Goedecker and J. Hutter, *Phys. Rev. B: Condens. Matter*, 1998, **58**, 3641-3662.
7. E. Mosconi, J. H. Yum, F. Kessler, C. J. G. Garcia, C. Zuccaccia, A. Cinti, M. K. Nazeeruddin,

- M. Grätzel and F. De Angelis, *J. Am. Chem. Soc.*, 2012, **134**, 19438-19453.
8. J. Yin, D. Cortecchia, A. Krishna, S. Chen, N. Mathews, A. C. Grimsdale and C. Soci, *J. Phys. Chem. Lett.*, 2015, **6**, 1396-1402.
9. Y. C. Kim, T. Y. Yang, N. J. Jeon, J. Im, S. Jang, T. J. Shin, H. W. Shin, S. Kim, E. Lee, S. Kim, J. H. Noh, S. I. Seok and J. Seo, *Energy Environ. Sci.*, 2017, **10**, 2109-2116.

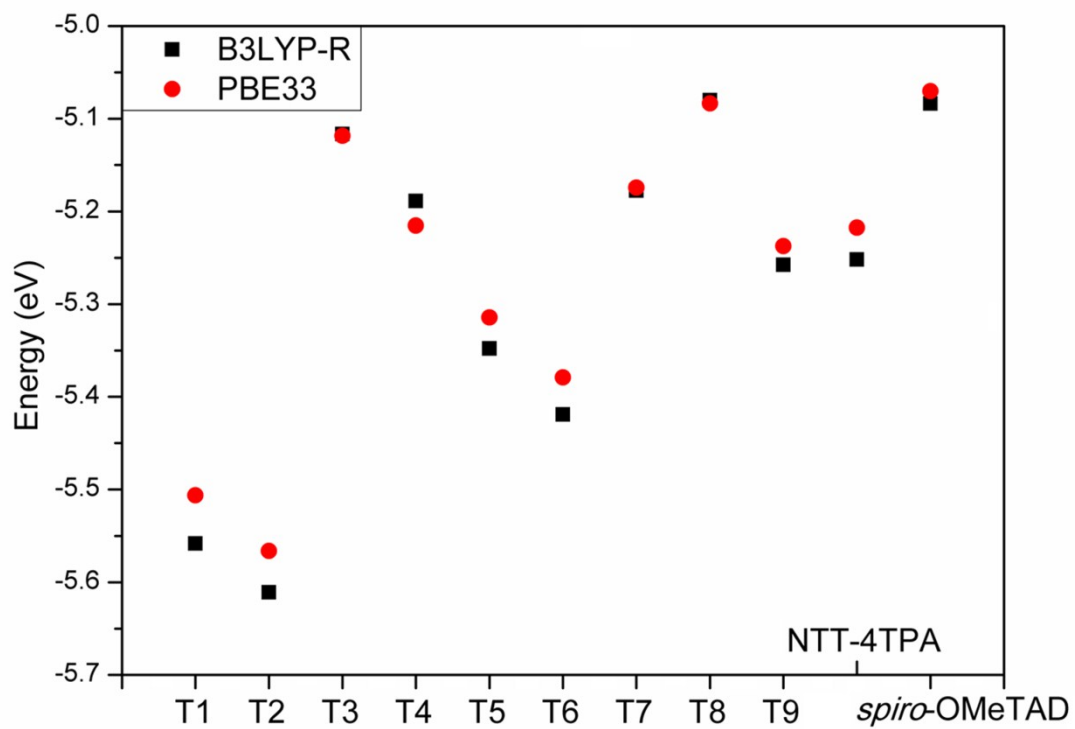


Fig. S1 Calculated HOMO levels of investigated molecules with the functional B3LYP and PBE33, and the B3LYP-R represents the data revised by a semi-rational formula.

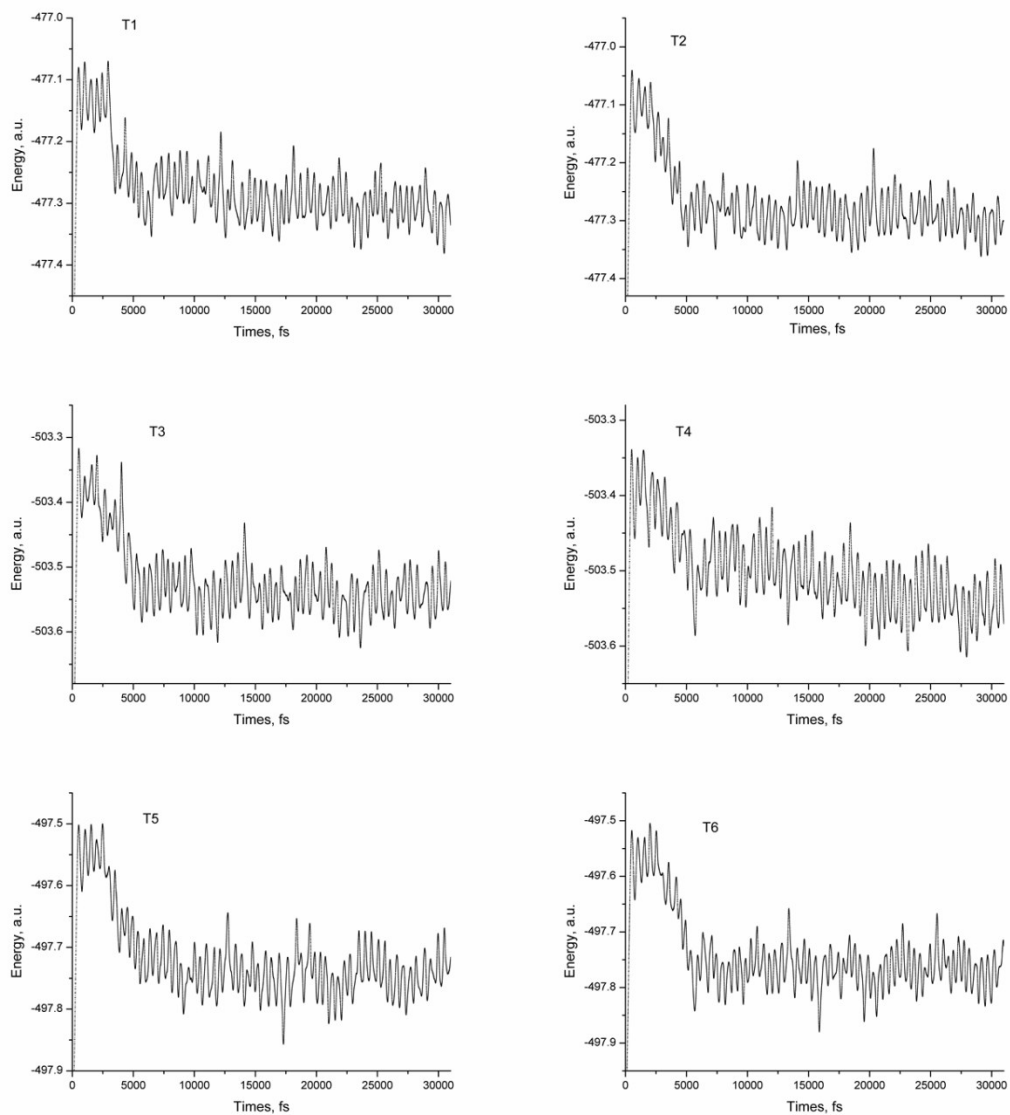


Fig. S2 Total electronic energy evolutions of the investigated dimers (T1~T6) as a function of simulation time.

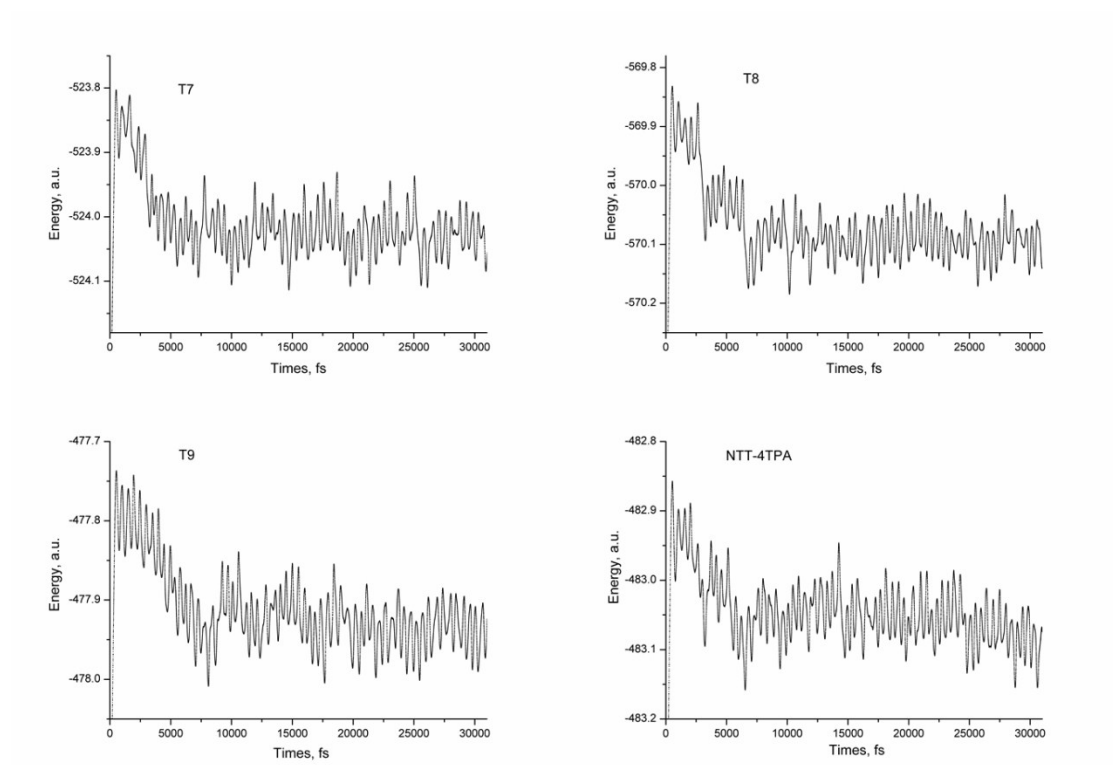


Fig. S3 Total electronic energy evolutions of the investigated dimers (T7~T9) as a function of simulation time.

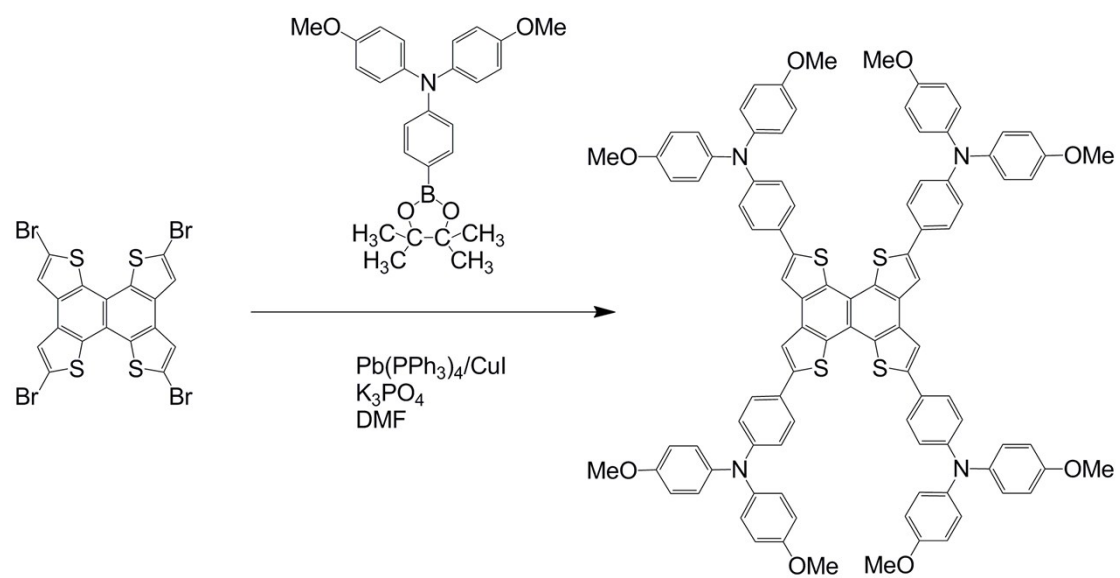


Fig. S4 Conjectural synthetic pathways for predicted molecules.

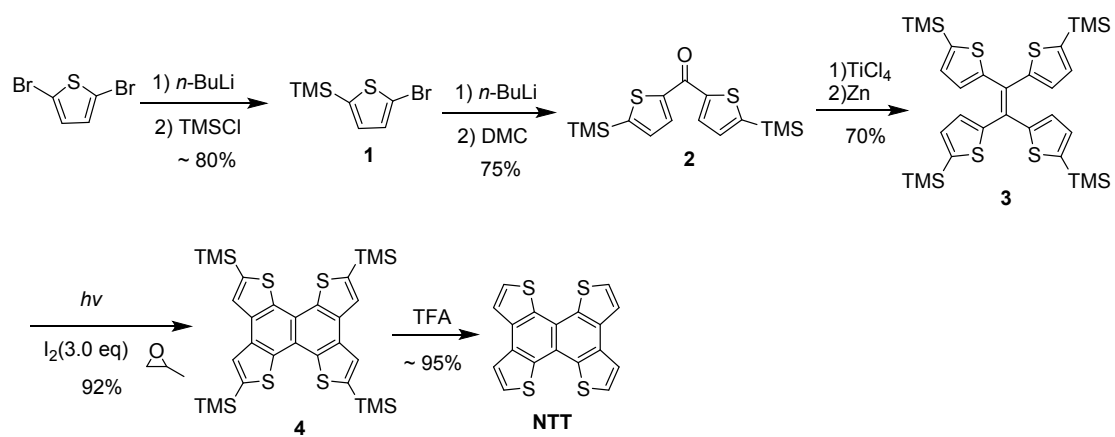


Fig. S5 Experimental synthetic pathways for the NTT core.

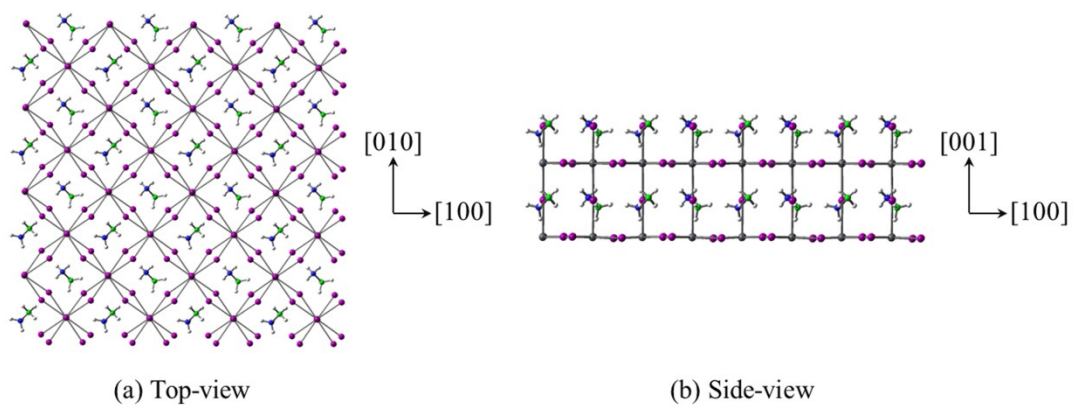


Fig. S6 Unrelaxed structure of the $(\text{MAPbI}_3)_{64}$ cluster with (001) surface exposed.

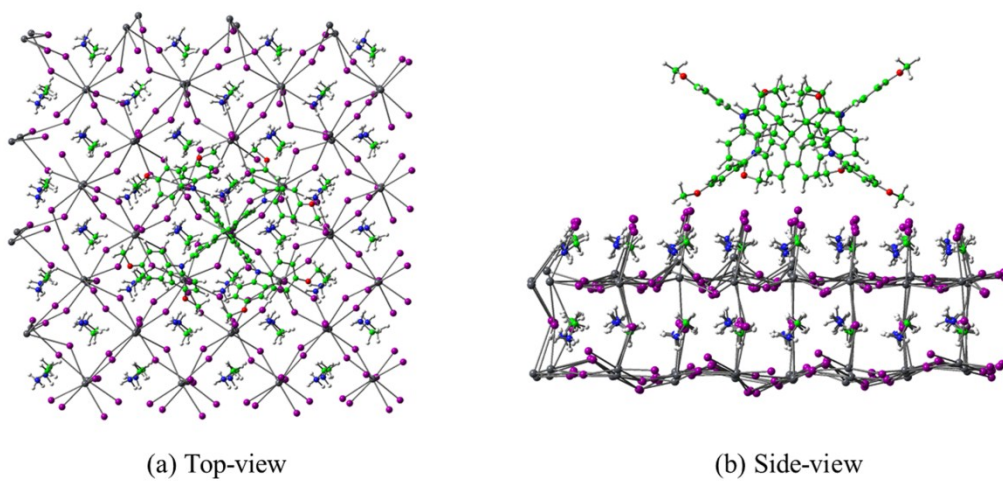
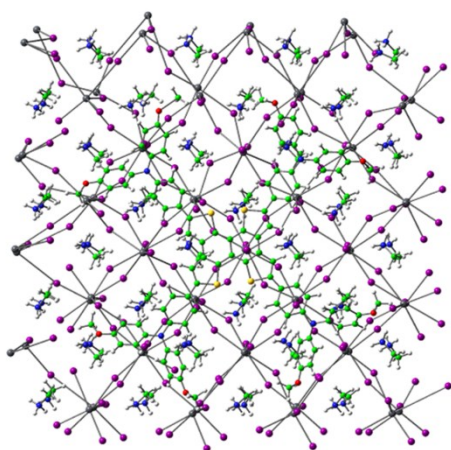
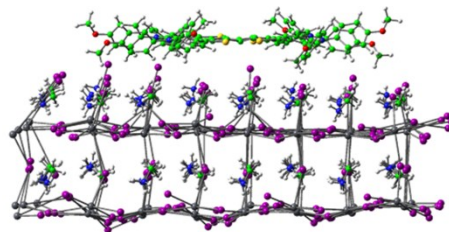


Fig. S7 Optimized geometry of the Spiro-OMeTAD/(MAPbI₃)₆₄ complex.



(a) Top-view



(b) Side-view

Fig. S8 Optimized geometry of the NTT-4TPA/(MAPbI₃)₆₄ complex.